A novel condensation reactor for efficient CO_2 to methanol conversion for storage of renewable electric energy

M.J. Bos, D.W.F. Brilman *

Sustainable Process Technology, Faculty of Science and Technology, University of Twente, PO Box 217, 7500 AE Enschede, The Netherlands

HIGHLIGHTS

- $CO_2 + H_2$ to methanol synthesis with near 100% CO_2 and H_2 efficiency.
- Reaction equilibrium bypassed via in situ condensation.
- High temperature reaction zone, low temperature condensation zone.
- Significant production rates achieved under natural convection conditions.
- Gas In, Liquid Out: no need for external recycle of gaseous reactants.

GRAPHICAL ABSTRACT
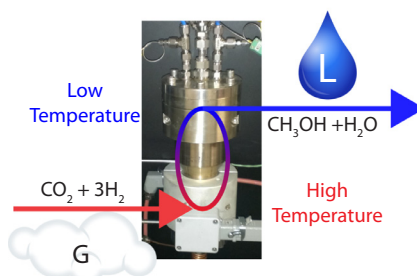
ABSTRACT

A novel reactor design for the conversion of CO_2 and H_2 to methanol is developed. The conversion limitations because of thermodynamic equilibrium are bypassed via in situ condensation of a water/methanol mixture. Two temperatures zones inside the reactor ensure optimal catalyst activity (high temperature) and full conversion by condensation at a lower temperature in a separate zone. Due to this full gas conversion there is no need for an external recycle of reactants. Experimental work confirmed full carbon conversion (>99.5%) and high methanol selectivity (>99.5% on carbon basis). Additionally, it was shown that due the temperature gradient inside the reactor significant reaction rates are achieved under natural convection conditions.

© 2014 Elsevier B.V. All rights reserved.

1. Introduction

In view of increasing production of renewable electric energy, a reliable and efficient storage method is desired, especially in view of the temporal mismatch between supply and demand. Methanol is one of the most promising potential storage media, storing the electric energy into an easy transportable, liquid fuel [1]. Moreover, it can be produced from the abundant available compounds CO_2 and water as input, next to the renewable electricity. Methanol is a versatile product since it can directly be used in fuels cells for electricity production and as a gasoline substitute. Furthermore

it can be upgraded to the diesel substituent dimethyl ether (DME) and chemical building blocks such as ethylene, propylene (MTO process) and syngas [2].

For the conversion of CO_2 and H_2O into methanol, the direct conversion route using CO_2 and H_2 was identified as more efficient than the routes via carbon monoxide. The main reason for this is that the thermodynamic minimum required energy to remove oxygen from either carbon dioxide or water is equal (Eqs. (1) and (2)). However, the conversion of CO_2 to CO has a low efficiency with the current state of technology [3], while producing the required hydrogen can be done with high efficiency via electrolysis [3].
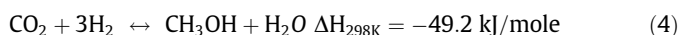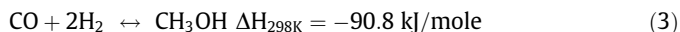
$$CO_2 \leftrightarrow CO + \frac{1}{2}O_2 \quad \Delta H_{298K} = 283 \text{ kJ/mole} \tag{1}$$
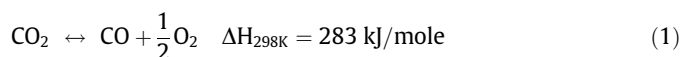
* Corresponding author. Tel.: +31 534896969.
E-mail address: d.w.f.brilman@utwente.nl (D.W.F. Brilman).

$$H_2O \leftrightarrow H_2 + \frac{1}{2}O_2 \quad \Delta H_{298K} = 286 \text{ kJ/mole} \qquad (2)$$

In literature two generic issues related to the production of methanol are mentioned. First, the exothermic character of the synthesis reaction implies a need for good temperature control [4], although the reaction of CO_2 with H_2 to methanol shown in Eq. (4) is less exothermic than the reaction starting from CO in Eq. (3). Secondly, and most important, thermodynamic equilibrium constraints induce a limited single pass conversion, especially when using CO_2 [5,6]. Which gains importance when the used CO_2 and H_2 are produced from more expensive and energy requiring renewable sources, increasing the need for processes with high selectivity and a high H_2 and CO_2 efficiency.

$$CO + 2H_2 \leftrightarrow CH_3OH \quad \Delta H_{298K} = -90.8 \text{ kJ/mole} \qquad (3)$$

$$CO_2 + 3H_2 \leftrightarrow CH_3OH + H_2O \quad \Delta H_{298K} = -49.2 \text{ kJ/mole} \qquad (4)$$

In this present work the thermodynamic limitations during the methanol synthesis from CO_2 and H_2 are discussed and a novel reactor design is proposed to circumvent these limitations, achieving high conversion and selectivity of the reactants to methanol.

2. Theoretical considerations

2.1. Methanol synthesis

During methanol synthesis the methanol formation reactions – Eqs. (3) and (4) – are in equilibrium with the water gas shift reaction, see in Eq. (5). Due to the exothermic character of the methanol formation reactions and the decrease of the number of moles during the reaction the equilibrium is more advantageous at high pressure and low temperature.

$$CO_2 + H_2 \leftrightarrow CO + H_2O \quad \Delta H_{298K} = 41.6 \text{ kJ/mole} \qquad (5)$$
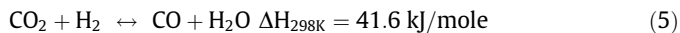
Chemical equilibria during the methanol synthesis are calculated using the equilibrium constants presented by Graaf et al. [7]. Nonideality of the gas mixture is taken into account by including the fugacity coefficients in the equilibrium constants, see Eqs. (6) and (7) where K is the equilibrium constant, T the temperature (K), ϕ the fugacity coefficient, y the gas phase mole fraction and P the pressure (bar). The fugacity coefficients are calculated by the modified Soave–Redlich–Kwong (mSRK) equation as described by Bennekom et al. [8]. Since, the original SRK equation is developed for hydrocarbon and slightly polar systems, the modified version for polar systems by Mathias [9] is used.

$$K_1 = 10^{\frac{5139}{T}} - 12.621 = \left[\frac{\phi_{CH_3OH}}{\phi_{CO}\phi_{H_2}^2}\right]\left[\frac{y_{CH_3OH}}{y_{CO}y_{H_2}^2 P}\right] \qquad (6)$$

$$K_2 = 10^{\frac{-2073}{T} + 2.029} = \left[\frac{\phi_{CO}\phi_{H_2O}}{\phi_{CO_2}\phi_{H_2}}\right]\left[\frac{y_{CO}y_{H_2O}}{y_{CO_2}y_{H_2}}\right] \qquad (7)$$

The equilibrium methanol yield is a function of pressure, temperature and feed composition, see Figs. 1 and 2. With increasing temperature the product composition is shifting from methanol rich to CO rich mixtures. Thereby, decreasing the carbon conversion to the methanol. The same trend is seen with decreasing pressure although the effect of decreasing pressure is smaller compared to the effect of increased temperature.

The equilibrium methanol yield of syngas based systems – see Fig. 1 – is significantly higher than of CO_2 feeds systems, see Fig. 2. If full conversion of reactants using CO_2 as feedstock is pursued, the increased recycling of unreacted components will increase operational and capital costs of the process. Therefore an advantaged method for shifting the equilibrium have to be
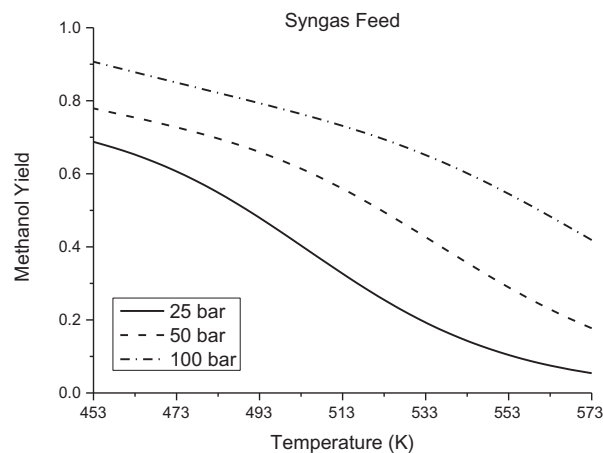

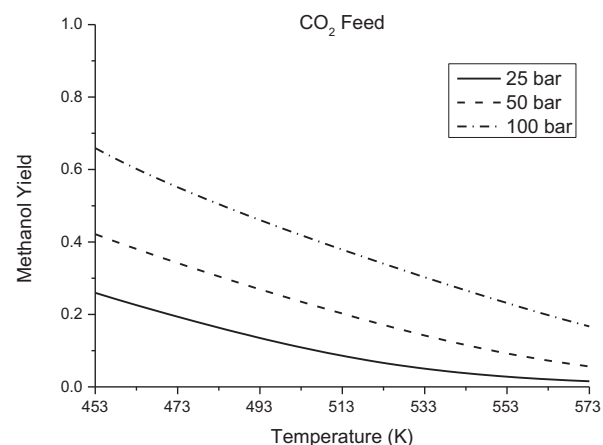**Fig. 1.** Chemical equilibria in methanol synthesis from syngas feed. Syngas feed: $H_2/CO/CO_2$ 75.9/16.9/7.2.

Fig. 2. Chemical equilibria in methanol synthesis from CO_2 feed. CO_2 feed: $H_2/CO/CO_2$ 75.0/0/25.0.

found. Several methods for shifting the equilibrium have been proposed in literature. For example, the equilibrium can be shifted by the use of membranes [10–12], using solvents such as n-dodecane [13], TEGDME [14] or alcohols [15]. Another way to shift the equilibrium is by condensation of the products vapors either by high pressure (200 bar) [16], very high pressure (>360 bar) [17], a radial temperature gradient [18] or a temperature gradient between a hot and a cold plate [19]. However, all these proposed methods introduce extra process steps, process equipment or increased capital cost due to high pressure equipment. Additionally, both designs using a temperature gradient do not achieve full reactant conversion in a single reactor pass and therefore an external recycle of reactant gases is still needed. Furthermore, both these temperature gradient designs have been verified with syngas feeds only. In this work, a novel reactor design achieving full CO_2 and H_2 conversion at low pressure is proposed. Full conversion at low pressure is achieved by condensation of product vapors using a temperature gradient and internal circulation inside the reactor.

2.2. Dew point temperature

To initiate condensation, the temperature of the condensation zone inside the reactor should be below the dew point temperature. Therefore, phase equilibria calculations are performed using the mSRK Equation of State [8,9]. During phase equilibrium the

fugacity of the liquid phase must be equal to the fugacity of the vapor phase, see Eq. (8) where y_i is gas phase mole fraction, ϕ_i^V the gas phase fugacity coefficient, x_i is liquid phase mole fraction and of ϕ_i^L the liquid phase fugacity coefficient, in all cases for the component i. The dew point temperature is the highest temperature for which Eq. (8) is valid for a certain gas composition and pressure.

$$y_i \phi_i^V = x_i \phi_i^L \tag{8}$$

In Fig. 3 it is shown that at high pressure (>100 bar) and low reaction temperature (473 K) condensation of the chemical equilibrium mixture can happen at the reaction temperature. However, with increased reaction temperature a significant higher pressure (>150 bar) is needed to condensate the equilibrium mixture at the reaction temperature. At relatively lower pressures (e.g. 50 bar) a decrease in temperature is needed to initiate condensation because the dew point temperature (403–413 K) is below the reaction temperature (473–533 K). Therefore, a temperature gradient should be present inside the reactor in order to initiate in situ condensation of product vapors.

2.3. Natural convection

Since a significant temperature gradient should be present inside the reactor this could result in a density gradient inside the reactor. Thereby, the reactor productivity can possibly be enhanced by a natural convection flow between condensation and reaction zones. Therefore, the density (ρ) of the equilibrium mixture generated at 503 K and 25/50/100 bar is calculated as a function of temperature (T) using the mSRK Equation of State [8,9], see Eq. (9) where P is the pressure (Pa), Z the compressibility and MW_i the mole weight of component i.

$$\rho(T) = \frac{P}{ZRT} \cdot \sum_{i=1}^{n} (y_i \cdot MW_i) \tag{9}$$

In Fig. 4 it can be seen that density is doubled when decreasing the temperature from 573 to 273 K. Furthermore, still a 35% density difference between the reaction temperature (503 K) and a condensing temperature of 373 K is present. The change in density is increasing with increased pressure due to increased non-ideality of the gas. Thereby, the difference in the compressibility factor (Z) is larger at high pressure than at low pressure. Since a temperature difference of at least 70 K between the reaction section (minimal 473 K) and the condensation section (maximal 403 K, see Fig. 3) should be present in the reactor, it is expected that the reactor design could benefit from natural convection phenomena.
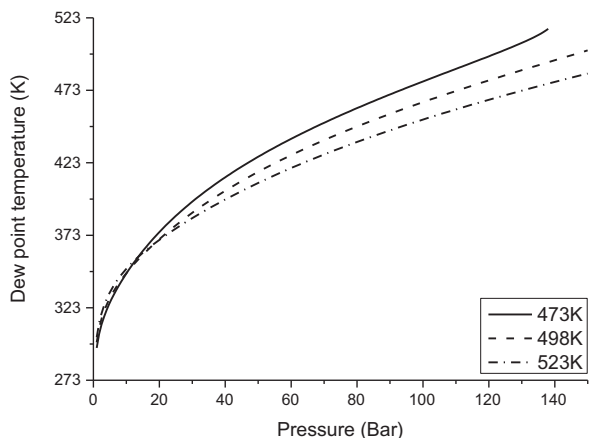

Fig. 3. Dew point of the equilibrium mixture at 473/498/523 K as a function of pressure. (CO_2 feed: $H_2:CO_2$ 3:1).
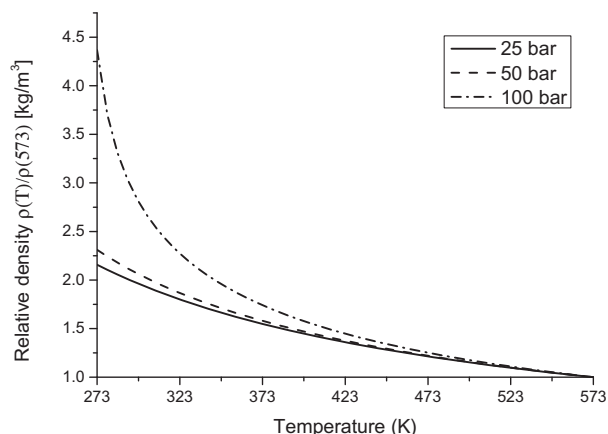

Fig. 4. Relative density ($\rho(T)/\rho(573\ K)$), calculated for the equilibrium composition generated at 503 K and resp. 25/50/100 bar (CO_2 feed: $H_2:CO_2$ 3:1).

2.4. Liquid-Out Gas-In Concept

According to the findings above a novel reactor design was designed and developed. In the novel reactor design two temperature zones are created inside the reactor in order to shift the chemical equilibrium. The catalyst zone operates at a higher temperature (473–533 K) to ensure optimal catalyst performance. In the second zone the temperature is lowered below the dew point temperature to condensate the products. In Fig. 5 is shown that the cold section is placed in top of the reactor, while reaction section is placed in the bottom of the reactor. In this way an optimal configuration is designed to benefit from natural convection flow. However, to ensure optimal reactor performance a fan is included.

The reactor is designed to operate in the so-called 'Liquid-Out Gas-In Concept' (LOGIC) modus. The gaseous reactants are fed and converted inside the reactor and accordingly the product vapors are condensed in situ and extracted from the reactor. In this way full conversion of gaseous H_2 and CO_2 reactants to the liquid products methanol and water can be achieved. Additionally, this concept makes possible carbon selectivity loss to CO in the reaction zone irrelevant, as CO will not leave the reactor as long as it is in the gas phase.

3. Experimental

3.1. Materials

Feed gas was supplied in a premixed bottle by Praxair, the Netherlands. Purity of the mixture was 24.8 vol% ± 2%rel. CO_2 in H_2
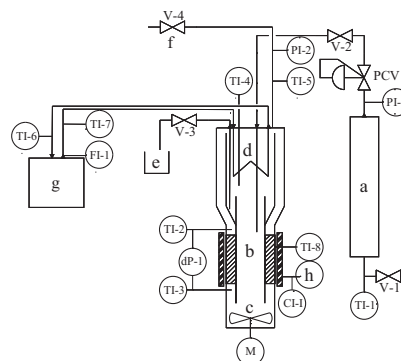

Fig. 5. Schematic overview of the setup: (a) buffer vessel, (b) catalyst section (annulus), (c) fan, (d) cooler, (e) liquid outlet, (f) purge, (g) water bath, (h) oven temperature controller, (TI) temperature indicator, (PI) pressure indicator, (CI) current indicator, (dP) differential pressure indicator, (FI) flow indicator, (PCV) pressure control valve, (V) valve.

(Feed gas 1) in the first experiment and 24.9 vol% ± 2%rel. CO_2 in H_2 (Feed gas 2) in the second experiment. The catalyst used was a commercial $Cu/ZnO/Al_2O_3$ catalyst (CP-488) provided by Johnson Matthey. The catalyst was provided and used in cylindrical tablets with 6 mm diameter and 5 mm length.

3.2. Set-up description

The setup consists of a buffer vessel, a reactor including an oven and a cooler and a water bath to regulate cooling temperature. A schematic overview of the setup is given in Fig. 5. Feed gas is fed to a 3.8 L buffer vessel (a) to a maximum pressure of 100 bar, which is measured by a pressure indicator (PI-1) [GE Druck, Unik PTX-5072-TB-A1-CA-H1-PA, 0–100 bar]. The pressure inside the reactor is measured by a pressure indicator (PI-2) [GE Druck, Unik PTX-5072-TB-A1-CA-H1-PA, 0–250 bar] and regulated by a pressure reducer (PCV) between the buffer vessel and the reactor.

The catalyst is placed in the annular spacing (b) of the bottom section of the reactor. The catalyst section has an inner diameter of 24 mm, an outer diameter of 48 mm and a length of 72 mm. The catalyst section is surrounded by a temperature controlled [Eurotherm, 2132] heating jacket (h). The current to the oven is measured by a current indicator (CI-1) [Phoenix Contact, MACX MCR-SL-CAC-5-I-UP]. The gas temperatures just before (TI-3) and after (TI-2) the catalyst bed is measured by K-type thermocouples [B + B sensors]. The pressure drop over the catalyst bed is measured by a differential pressure indicator (dP-1) [GE Druck, LPM-9481]

A fan (c) of 38 mm diameter is installed to ensure circulation inside the reactor. The fan is powered by a 30 W magnetic coupled motor (M) to ensure a gas-tide power transmission. The cooler (d) is placed in the inner part of the top section and it is constructed from spiral wounded copper tubing. Gas temperatures of the cooler inlet (TI-5) and outlet (TI-4) are measured by K-type thermocouples [B + B sensors]. The cooler is operated with tap water and the temperature is regulated by a water bath (g) [Julabo F34-HE]. The water flow is measured by a flow indicator [POM B.I.O-Tech Becker 52.01 in combination with Red Lion IFMA 0035] and the water inlet (TI-7) and outlet temperature (TI-6) is measured by K-type thermocouples [B + B sensors]. Liquid product is collected inside the reactor in a collection cup with a volume of approximate 6 mL. The product is tapped from the reactor into ice-cooled collection bucket (e) outside the reactor.

3.3. Experimental procedure

The reactor was filled with a catalyst and activated according to the procedure provided by the manufacturer. In between experiments the reactor is stored under a reducing environment. Before an experiment the buffer vessel was filled with feed gas from the gas bottle and the reactor is purged with the feed gas. After purging the reactor it was pressurized and heated, the catalyst outlet temperature was regulated by the temperature of the oven. The cooler was turned on and the cooler outlet temperature was controlled by the flow and temperature of the cooling water. The fan was switched on and the fan speed was controlled by the supplied voltage.

The experiments were performed in semi-continuous mode, a continuous amount of feed gas was fed from the buffer vessel to the reactor in order to maintain the reactor pressure at 50 bar, since the pressure in the reactor will decrease due to reaction and condensation. At every two bar of pressure drop in the buffer vessel the condensate was tapped from the reactor resulting in approximate 4 mL of condensate. The productivity of the reactor was measured by the liquid production per unit of time. Productivity was

determined over a minimum of 5 condensate samples under stable conditions.

During the condenser temperature experiments the condenser temperature is varied between 358 K and 413 K. The reactor pressure is kept constant at 50 bar and the catalyst outlet temperature is regulated at 483 K. The fan speed was adjusted (via power supply voltage, between 8 and 10 V) to maintain a constant pressure drop over the catalyst bed of 0.15 mbar. It is expected that a constant pressure drop over the catalyst bed reflects a constant circulation flow inside the reactor. However, no method of direct flow measurement was present at the reactor.

The fan speed was varied between 0 and 10 V during the fan speed experiments. The catalyst bed outlet temperature was regulated at 468 K and the cooler outlet temperature was 363 K. The reactor pressure was maintained at 50 bar.

The liquid product was analyzed in a HPLC [Agilent Technologies 1200 Series] using RID detection and 300 mm × 7.7 mm Hi-Plex H column equipped with a pre-column. The injected volume was 10 µL, the temperature 65 °C and the mobile phase 5 mM H_2SO_4 at 0.6 mL/min. Calibration curves were obtained by injecting mixtures of known composition in the range of interest before the samples.

4. Results and discussion

Two series of experiments have been performed. In the first set the condenser section outlet temperature has been varied, while in the second set the fan speed is varied. The goal of the first set of experiments is 'proof of concept' of the Liquid-Out Gas-In Concept (LOGIC), showing full conversion and high selectivity of the concept. In the second set of experiments the effect of fan speed is tested, showing the performance under natural convection flow.

4.1. Condenser temperature

In Fig. 6 is shown that the reactor productivity increases with a decreasing condenser temperature. At a lower condenser temperature a larger fraction of the product vapors will condense and thereby a larger conversion per pass can be achieved in the catalyst section. The productivity reaches zero for a condenser temperature of about 418 K which approaches the calculated dew point temperature of the equilibrium composition as shown in Fig. 3. Accordingly, it is shown that the system reaches the equilibrium composition for high condenser temperatures.
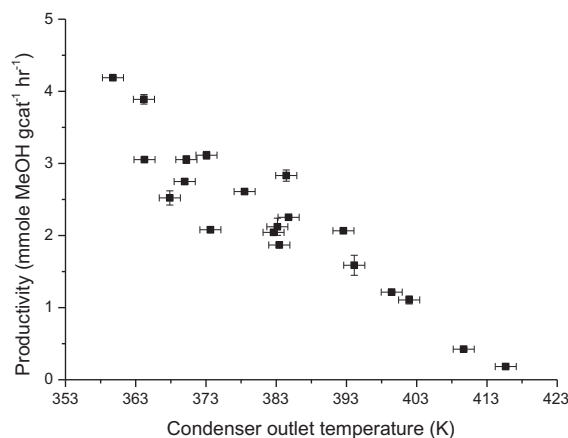

Fig. 6. Reactor productivity as a function of condenser outlet temperature. (P = 50 bar, catalyst bed outlet temperature = 483 K, Catalyst bed pressure drop = 0.15 mbar, Feed gas 1).

The condensate composition is found to be 48.4 ± 2.0 mol% of methanol in water, whereas the expected theoretical ratio is 50 mol% methanol in water. However, we expect, as methanol is more volatile than water, that possibly some methanol is evaporated during sampling. Additionally, extra water can be produced by the water gas shift when some gas (possible containing CO) is lost during liquid sampling. No significant changes in liquid composition are seen for changes in condenser temperature. At the prevailing conditions in the catalyst zone, the formed methanol is for more than 99.5 mol% pure and only traces of ethanol, 1-propanol and formic acid are found.

Because no gas phase is subtracted from the reactor a very high carbon yield of larger than 99.5% is found. Mass balances based on the pressure decrease in the buffer vessel and the recovered condensate are consistent (within few percent).

4.2. Fan speed

The novel design is able to produce methanol condensate at a significant production rate without forced convection by the fan, see Fig. 7. Thereby, proving that the concept can operate with moving parts inside the reactor. Hence opening the potential for a simple small-scale and standalone methanol producing vessel. This set of experiments achieved the same high carbon yield to methanol as the previous set. The average methanol concentration is 47.5 ± 0.6 mol% of methanol in water, again only traces of ethanol and formic acid are detected leading to a methanol purity of >99.8%.

It should be mentioned that determination of the absolute flows inside the reactor was not possible because the pressure drop over the catalyst bed was too low (<0.1 mbar) to measure with the available equipment. Therefore, relative fan speed in the form of the applied voltage to the fan is presented in the figures below.

At low fan speeds the productivity is increased in comparison to natural convection. This is probably the effect of enhanced mass transfer from and to the catalyst and condenser by forced convection. Thereby, the catalyst is used more efficiently. However, further enhancement of mass transfer by increased fan speed showed decreasing productivity. A reason for this behavior can be found when the gas temperatures of the inlet and outlet of the catalyst bed are compared, see Fig. 8. It is seen that at higher flows the gas temperature of catalyst bed inlet drops significant, thereby reducing the average catalyst temperature and consequently reducing the reaction rates. Apparently, at lower fan speed internal heat transfer is sufficient to preheat the gas to the catalyst bed to a temperature close to the catalyst bed outlet temperature
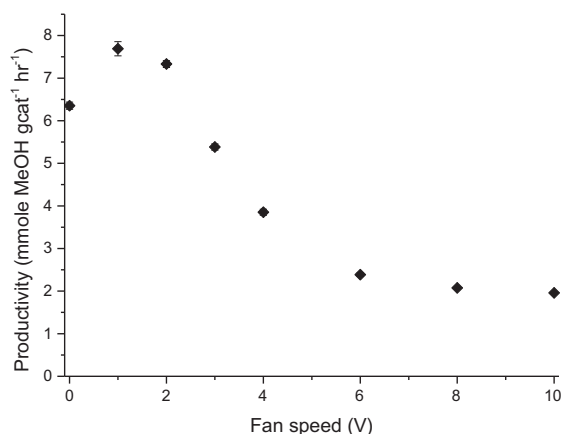
(which is used as set point for the catalyst heater). At higher flow rates additionally heat transfer is necessary to preheat the gas and increase catalyst efficiency. To improve radial heat transfer from the catalyst bed to the inner tube – containing the cold recycling gas returning to the catalyst – one may consider the use of conductive structured catalyst as recently discussed by Montebelli et al. [20]. Additionally, it is seen that the condenser outlet temperature still matches its set value thereby suggesting that cooling rates are still sufficient at high flow rates.

At high fan speed it is seen that the flow inside the reactor is too high to maintain catalyst temperature and reaction kinetics. Additionally, it is seen that in the previous set of experiments – presented in Fig. 6 – the flow was also too high since the catalyst inlet temperature was relatively low (393–413 K). An effect of the catalyst bed outlet temperature is seen when comparing the productivity at high fan speed in Fig. 7 (2 mmole MeOH gcat^{-1} h^{-1}, catalyst out 468 K) with the higher productivity in Fig. 6 at the same condenser temperature of 363 K (3–4 mmole MeOH gcat^{-1} h^{-1}, catalyst out 483 K).

It is clear that reactor productivity can be further increased by optimizing flow and catalyst temperature. By increasing the catalyst inlet temperature the productivity of the reactor is increased. In the current setup and the used low catalyst outlet temperature the most optimal catalyst inlet temperature is achieved at low flow. This optimal flow can be increased by increasing the gas temperature of the catalyst bed inlet, for example by increased internal heat transfer or by an additional heat source. It is expected that by increasing the catalyst bed outlet temperature – thereby increasing the average catalyst temperature – the optimal flow is expected to also increase since the reaction rates will increase.

4.3. Energy efficiency

The reactor energy efficiency is decreasing with increased fan speed (see Fig. 9) because more energy input is needed while the productivity is decreasing. The difference between the cooler and oven duty is a measure of the heat loss (123 ± 45 W) of the reactor. The maximum produced reaction heat is 8.5 W and not very significant compared to the oven duty in this laboratory setup.

In this small lab setup, the energy input per kg MeOH is too high under the current condition (see Fig. 10), because it is about three-times the higher heating value of methanol (22.4 MJ/kg [4]). However, this energy input includes heat loss to the environment and
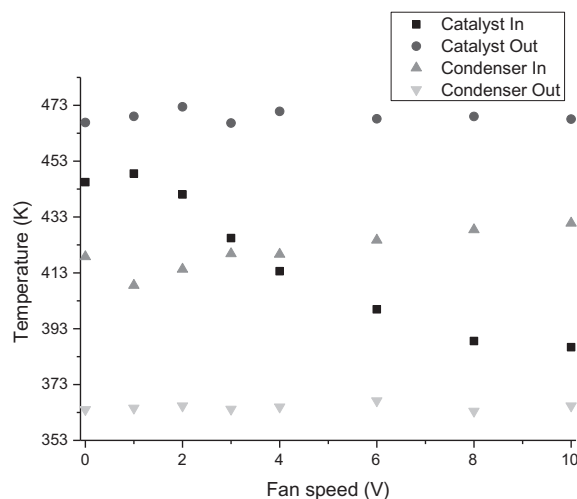

Fig. 7. Reactor productivity as a function of fan speed. (P = 50 barg, catalyst bed outlet temperature = 268 K, condenser outlet temperature = 363 K, feed gas 2).

Fig. 8. Gas temperatures at the catalyst and condenser inlet/outlet as a function of fan speed. (P = 50 barg, catalyst bed outlet temperature = 468 K, condenser outlet temperature = 363 K, feed gas 2).
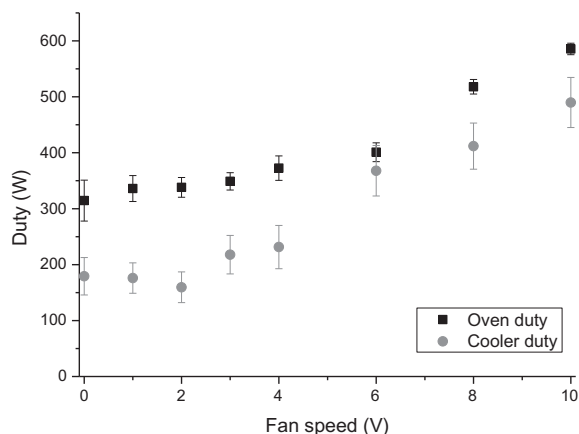
Fig. 9. Oven and cooler duty as a function of fan speed. (P = 50 barg, catalyst bed outlet temperature = 468 K, condenser outlet temperature = 363 K, feed gas 2).
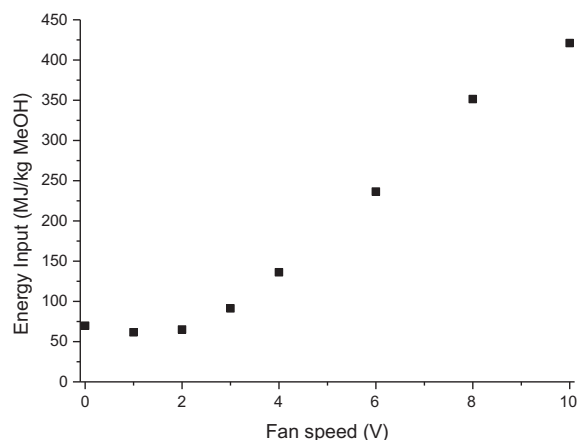

Fig. 10. Energy input per kg of methanol as a function of fan speed. (P = 50 barg, catalyst bed outlet = 468 K, condenser outlet temperature = 363 K, feed gas 2).

the loss of the cooling duty. If the heat loss to environment is neglected (to be achieved by an improved design) and 50% of the condenser duty is used to reheat the cold gas, the energy input at low fan speeds is already reduced to the higher heating value of methanol. This underlines the importance of further work on heat exchange in this reactor design.

5. Conclusion

A novel reactor design to shift the equilibrium during methanol synthesis is developed. By the creation of two temperature zones, in situ condensation of the products vapors is possible at low pressure thereby shifting the equilibrium. The design of the reactor consisted of a cold condensation zone in the top and a hot reaction zone in the bottom of the reactor in order to be able to benefit from natural convection phenomena.

Experimental results showed that indeed methanol was produced with the novel 'Liquid Out Gas In Concept' reactor. The expected 50/50 M ratio of water/methanol was approached in the produced condensate. The carbon yield to methanol was very high (above 99.5%), since the obtained methanol contained only traces of ethanol, 1-propanol and formic acid.

Additional experiments with varying fan speed showed that indeed a significant methanol production was found without forced convection, opening the potential for a simple small-scale and standalone methanol producing vessel.

The energy efficiency of the current lab scale setup is too low to produce methanol with a positive energy balance. Therefore more work is needed in optimizing the conditions inside the reactor, heat exchange between the hot and cold section inside the setup and minimizing heat loss to the environment.

References

[1] G.A. Olah, A. Goeppert, G.K.S. Prakash, Chemical recycling of carbon dioxide to methanol and dimethyl ether: from greenhouse gas to renewable, environmentally carbon neutral fuels and synthetic hydrocarbons, J. Org. Chem. 74 (2008) 487–498.
[2] M. Bertau, H. Wernicke, F. Schmidt, Methanol utilisation technologies, in: M. Bertau, H. Offermanns, L. Plass, F. Schmidt, H.-J. Wernicke (Eds.), Methanol: The Basic Chemical and Energy Feedstock of the Future, Springer, Berlin Heidelberg, 2014, pp. 327–601.
[3] C. Graves, S.D. Ebbesen, M. Mogensen, K.S. Lackner, Sustainable hydrocarbon fuels by recycling CO_2 and H_2O with renewable or nuclear energy, Renew. Sustain. Energy Rev. 15 (2011) 1–23.
[4] E. Fiedler, G. Grossmann, D.B. Kersebohm, G. Weiss, C. Witte, Methanol, in: Ullmann's Encyclopedia of Industrial Chemistry, Wiley-VCH Verlag GmbH & Co. KGaA, 2000.
[5] D. Mignard, C. Pritchard, Processes for the Synthesis of liquid fuels from CO_2 and marine energy, Chem. Eng. Res. Des. 84 (2006) 828–836.
[6] B. Doss, C. Ramos, S. Atkins, Optimization of methanol synthesis from carbon dioxide and hydrogen: demonstration of a pilot-scale carbon-neutral synthetic fuels process, Energy Fuels 23 (2009) 4647–4650.
[7] G.H. Graaf, P.J.J.M. Sijtsema, E.J. Stamhuis, G.E.H. Joosten, Chemical equilibria in methanol synthesis, Chem. Eng. Sci. 41 (1986) 2883–2890.
[8] J.G.v. Bennekom, J.G.M. Winkelman, R.H. Venderbosch, S.D.G.B. Nieland, H.J. Heeres, Modeling and experimental studies on phase and chemical equilibria in high-pressure methanol synthesis, Ind. Eng. Chem. Res. 51 (2012) 12233–12243.
[9] P.M. Mathias, A versatile phase equilibrium equation of state, Ind. Eng. Chem. Process Des. Dev. 22 (1983) 385–391.
[10] A.G.J.v.d. Ham, H.v.d. Berg, A. Benneker, G. Simmelink, J. Timmer, S.v. Weerden, Hydrogenation of carbon dioxide for methanol production, Chem. Eng. Trans. 29 (2012) 181–186.
[11] F. Gallucci, L. Paturzo, A. Basile, An experimental study of CO_2 hydrogenation into methanol involving a zeolite membrane reactor, Chem. Eng. Process. 43 (2004) 1029–1036.
[12] R.P.W.J. Struis, S. Stucki, Verification of the membrane reactor concept for the methanol synthesis, Appl. Catal. A 216 (2001) 117–129.
[13] K. Hagihara, H. Mabuse, T. Watanabe, M. Kawai, M. Saito, Effective liquid-phase methanol synthesis utilizing liquid–liquid separation, Energy Convers. Manage. 36 (1995) 581–584.
[14] C. Krishnan, J.R. Elliott, J.M. Berty, Continuous operation of the Berty reactor for the solvent methanol process, Ind. Eng. Chem. Res. 30 (1991) 1413–1418.
[15] B. Xu, R. Yang, F. Meng, P. Reubroycharoen, T. Vitidsant, Y. Zhang, Y. Yoneyama, N. Tsubaki, A new method of low temperature methanol synthesis, Catal. Surv. Asia 13 (2009) 147–163.
[16] J.G. van Bennekom, R.H. Venderbosch, J.G.M. Winkelman, E. Wilbers, D. Assink, K.P.J. Lemmens, H.J. Heeres, Methanol synthesis beyond chemical equilibrium, Chem. Eng. Sci. 87 (2013) 204–208.
[17] B. Tidona, C. Koppold, A. Bansode, A. Urakawa, P. Rudolf von Rohr, CO_2 hydrogenation to methanol at pressures up to 950 bar, J. Supercrit. Fluids 78 (2013) 70–77.
[18] B. Haut, V. Halloin, H. Ben Amor, Development and analysis of a multifunctional reactor for equilibrium reactions: benzene hydrogenation and methanol synthesis, Chem. Eng. Process. 43 (2004) 979–986.
[19] D. Perko, A. Pohar, J. Levec, Hydrogenation of CO_2 and CO in a high temperature gradient field between catalyst surface and opposite inert cool plate, AIChE J. 60 (2014) 613–622.
[20] A. Montebelli, C.G. Visconti, G. Groppi, E. Tronconi, S. Kohler, Optimization of compact multitubular fixed-bed reactors for the methanol synthesis loaded with highly conductive structured catalysts, Chem. Eng. J. 255 (2014) 257–265.